Solid Freeform Fabrication 2019: Proceedings of the 30th Annual International
Solid Freeform Fabrication Symposium – An Additive Manufacturing Conference
Reviewed Paper

Frequency Inspection of Additively Manufactured Parts for Layer Defect Identification

Aimee Allen[1], Kevin Johnson[1], Jason Blough[1], Andrew Barnard[1], Troy Hartwig[2], Ben Brown[2], David Soine[2], Tristan Cullom[3], Douglas Bristow[3], Robert Landers[3], Edward Kinzel[4]

[1]Department of Mechanical Engineering-Engineering Mechanics, Michigan Technological University, Houghton, MI 49931

[2]Honeywell Kansas City National Security Campus, Kansas City, MO 64147

[3]Department of Mechanical Engineering and Aerospace, Missouri University of Science and Technology, Rolla, MO 65401

[4]Department of Aerospace and Mechanical Engineering, University of Notre Dame, Notre Dame, IN 46556

Abstract

Additive manufactured (AM) parts are produced at low volume or with complex geometries. Identifying internal defects is difficult as current testing techniques are not optimized for AM processes. The goal of this paper is to evaluate defects on multiple parts printed on the same build plate. The technique used was resonant frequency testing with the results verified through Finite Element Analysis. From these tests, it was found that the natural frequencies needed to detect the defects were higher than the excitation provided by a modal hammer. The deficiencies in this range led to the development of other excitation methods. Based on these results, traditional methods of resonant part inspection are not sufficient, but special methods can be developed for specific cases. This work was funded by the Department of Energy's Kansas City National Security Campus which is operated and managed by Honeywell Federal Manufacturing Technologies, LLC under contract number DE-NA0002839.

1. Introduction

Additive manufactured parts have an advantage over traditional casting methods when considering parts produced at a low volume or parts with complex geometries. As the industry for additive manufacturing increases, new challenges become present. One of these challenges is part integrity. Defects on the surface of AM parts can be identified visually. Internal defects are more difficult to find as they cannot be seen by the naked eye.

The AM process considered in this paper is selective laser melting (SLM). SLM is a 3-D printing process where a laser sinters each layer of metal powder to form 3-D printed metal parts. One internal defect that occurs from this process is a laser penetration defect or voids. Voids are holes in a part that occur in SLM when the laser misses sintering a layer or layers.

The current methods for inspecting internal defects, such as voids, include computed tomography (CT) scanning and x-ray. CT and x-ray testing are effective methods for detecting internal defects [1]. However, these methods take time to perform and can come at a high cost as

CT and x-ray testing are not optimal for AM part inspection during and after processing [2]. Dynamic testing is a quick and low-cost method of testing for defects. The elimination of defects before CT and x-ray can save both time and money [3].

Dynamic testing includes both shaker and impact (modal) hammer testing. AM parts excited by these methods will vibrate at their natural frequencies. Natural frequencies, or resonances, are structural properties defined by mass, stiffness, damping, and boundary conditions for the structure [4].

Near the resonance of the structure, the response amplitude will be higher than the other frequencies. The peaks on a Frequency Response Function (FRF) indicate the frequency at which a resonance occurs. An FRF relates the input to the output of two measurement points on a structure [4]. The input for an FRF is usually a force with the output being displacement, velocity, or acceleration. One metric in which FRFs are often evaluated to determine if the measurement was "good" is by evaluating the coherence. The coherence is the amount of output directly related to the input. If all the input is directly related to the output the response is equal to one, if none of the input is related to the output the response is equal to zero.

The FRF peaks can be represented by mode shapes. A mode shape is the physical representation of a natural frequency. For example, as suggested by Johnson et al., if a guitar string is plucked the 1st mode shape is the entire string vibrating and the 2nd mode shape is the string split in two with a node in the middle and the string moving on both sides of it. Mode shapes become increasingly more complex as frequency increases. Due to this effect, the capability of finding tiny defects increases.

Structures with the same material properties and boundary conditions will have the same natural frequencies and mode shapes. If the material properties or boundary conditions change, the peaks in the FRF will shift in frequency. A part containing a defect can be distinguished from good parts if its natural frequency is outside the standard deviation from a collection of good parts [3].

Free-free boundary conditions are often the approach used to dynamically test structures. Free-free is suspending the structure on bungies or placing the structure on foam. By supporting the structure in free-free conditions, the modes from supporting structures, such as a fixture, are eliminated. Due to the increased cost and time of separating individual pieces for testing, the parts tested in this paper use a fixed boundary condition.

Johnson et al. performed similar testing on chimney specimens. The authors concluded that "dynamic evaluation method has significant potential to find 'bad' parts," but further testing is needed before dynamic evaluation is commercialized.

This article expands on the dynamic evaluation by Johnson et al. by considering a greater number of parts with increased complexity. Specifically, the research question investigated is "What size layer defects can be detected in 316L Stainless Steel parts attached to the same build plate?" The parts tested in this article were analyzed to determine if nominal groups of parts and

groups with different amounts of defect could be separated from each other through resonant frequency testing.

2. Methods

Part testing was the same as Johnson et al. except a small impact hammer and no Digital Image Correlation (DIC) were used. The small impact hammer was used as the parts were more closely spaced and smaller in size than the parts tested by Johnson et al. No digital image correlation was used since the initial shaker testing did not provide enough dynamic excitation nor distinct FRF peaks when recorded with a Scanning Laser Doppler Vibrometer (SLDV). The frequency range of interest for the parts tested in this paper were above the excitation range of the shaker. Additionally, Finite Element Analysis was used to validate the results from the experimental testing.

The first set of parts tested was a build plate of 45 tensile bars provided by our research partner Missouri University of Science and Technology (MS&T). These tensile bars were split into nine groups of five. One group was nominal parts with the rest of the groups having a variation of the same layer defect. This layer defect was a result of intentional missing laser sintering layers of powder. The shape of the defect was rectangular, representative of the geometry of the tensile bar (Fig. 1a). This layer defect ranged from 50 to 400 μm and was located approximately 1/3 of the way up from the bottom of each tensile bar (Fig. 1b). The defect increased in height for each subsequent group.

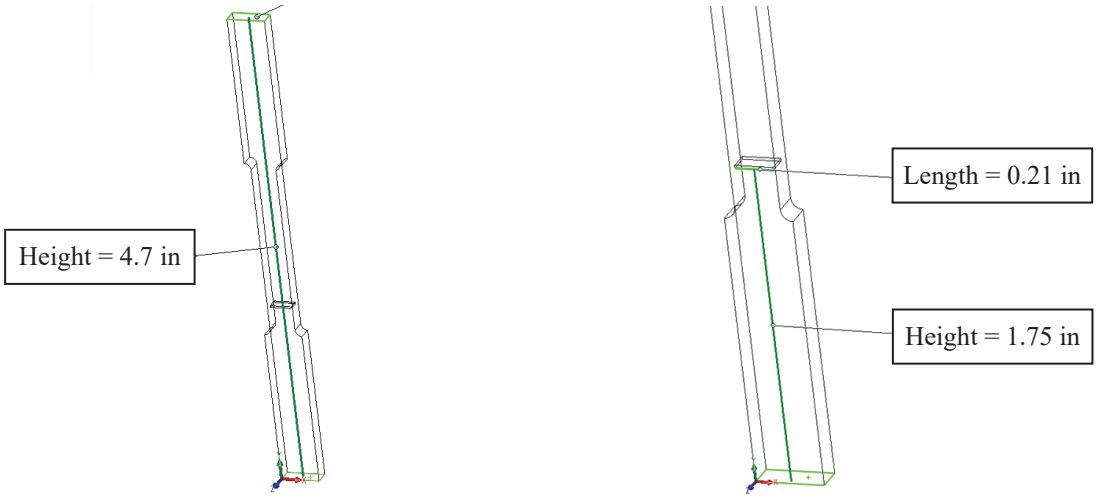

Figure 1: Height of tensile bar (1a) and defect length and height from base (1b)

MTU was not informed which groups had each size defect until after testing and presentation to the sponsor. The groups labeled 1-9 are shown from the top view of the build plate (Fig. 2a). The groups were randomly placed on the build plate to ensure no groups were congregated together. The bars were numbered for identification (Fig. 2b). These parts were not printed with the supporting structure. The supporting structure assists in printing the specimen and is removed from the build plate in post-processing.

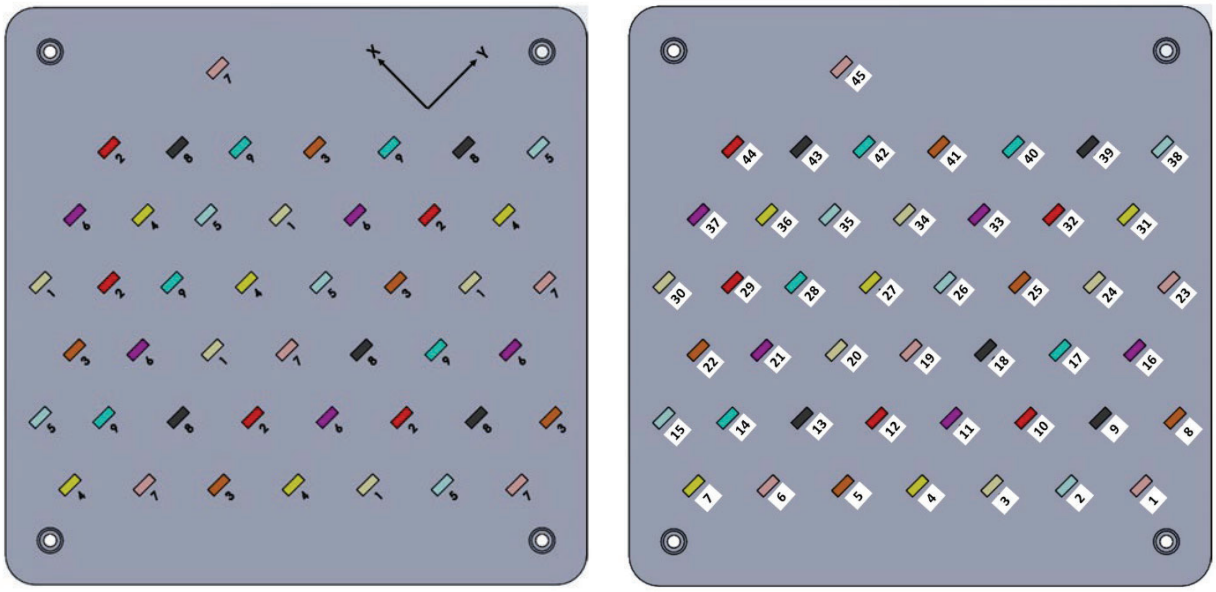

(2a) (2b)

Figure 2: Layer defect build with one group at nominal and the other eight with varied amount of layer defects provided by MS&T

The printed layer defect build tested is shown in (Fig. 3). Coupling between parts occurs when parts are located near each other connected to the same structure. Weights were added to each of the bars not being impacted to eliminate the effect of coupling in the response. Each bar was impacted in the −X – direction with the SLDV recording the velocity response from the +X – direction. As only the x-direction of each cantilever beam was tested, the only modes that the results should display are x-axis bending modes. This means there should be no axial or y-axis bending modes in the experimental results. There is a possibility for some torsional modes to appear if the hammer impact was not directly in the center of the cantilever. The impact being off-center would cause some twisting in the structure producing a small torsional response.

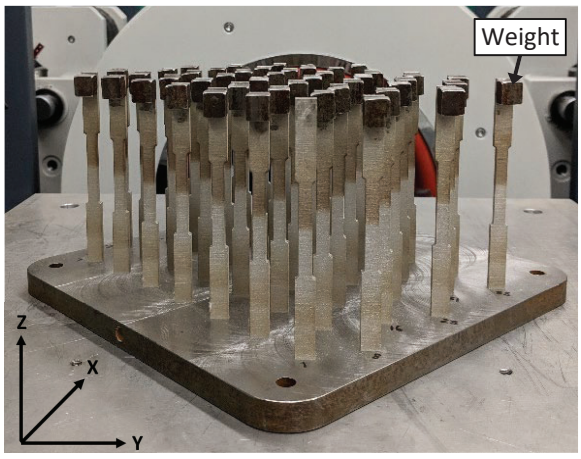

Figure 3: Layer defect build with weights

The FEA modeling parameters consisted of modeling each individual bar on the plate. Each bar was fixed in the model where the bar connected to the build plate. Each bar was evaluated for up to 20 mode shapes.

The next build plate provided to MTU was another forest tensile bar build with all the bars being nominal. This plate was tested in the same way as the first plate with the placement of each of the bars held the same. The purpose of testing this plate was to analyze the variation in the printing of the tensile bars and compare the results with the build plate with layer defects.

The last build plate was three topology optimized brackets (Fig. 4). These parts were printed without defects in order to analyze whether the parts could be tested and if they compared to the FEA results performed on them. If the parts could be tested and compared to the FEA, then defects would be added and analyzed. These parts were printed with the supporting structure since printing without the supporting structures failed. These specimens were tested in the ears at the top of the structure. The hammer direction and SLDV were oriented in the same direction as the forest bar builds.

The FEA performed on the brackets was provided by Missouri S&T. The parameters for the FEA are similar to the forest bar builds. The boundary condition for the brackets was fixed to the plate. The first eight modes were calculated from the FEA.

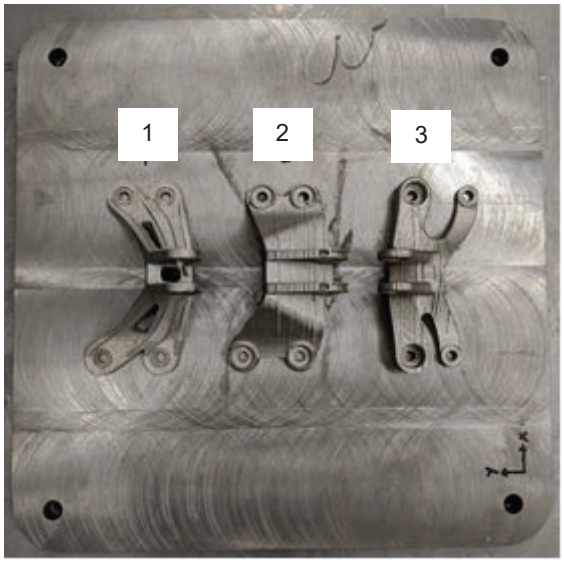

Figure 4: Topology Optimized Brackets indicated by number provided by MS&T

3. Results

1.1 Layer Defect Build

A resonant frequency test was performed to determine whether the 9 groups with defects could be distinguished from each other. These four modes, Mode 1, Mode 3, Mode 5, and Mode 8 were clearly distinguished from the resonant frequency test; whereas the other modes listed were determined from FEA (Fig. 5a). These four modes indicate the first four bending modes on

the x-axis of the structure. There were no distinct bar groupings that could be visually identified (Fig. 5b and Fig. 5c). This indicates further testing is needed to determine if the groups can be distinguished. An interesting observation from this testing is that as the mode number increased there was a larger span between natural frequencies and more damping (wider peaks).

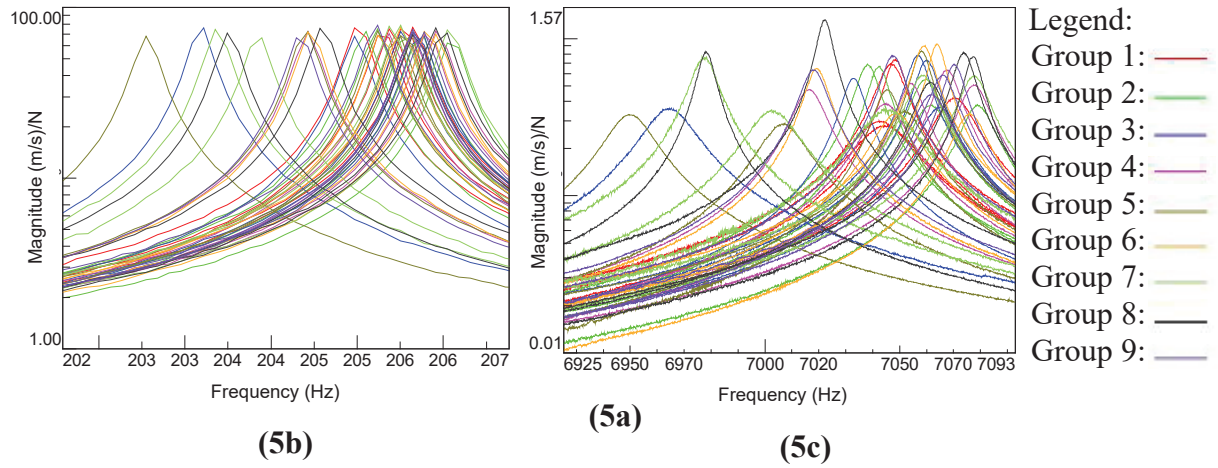

Figure 5: FRFs of the all bars on the defect build (5a), FRF at the 200 Hz mode (5b) and 7050 Hz mode (5c)

The average and three-sigma for the bar groups from the first four bending modes was performed to establish if the defect groups could be separated. The three-sigma for the nominal group on the build was compared to the other 8 groups with defects (Table 1). Since none of the other bar group's natural frequencies (not shown) fell outside the three-sigma limits this indicates that no significant statistical difference was observed between the groups. This observation indicates that the natural frequencies of the bars from each group overlap other bar groupings and no individual defect groups were detected.

Table 1: Three-sigma values for Group 1: Nominal parts on forest build

Mode No.	Natural Frequency (Hz)	three-sigma (Hz)
Mode 1	205.35	± 0.69
Mode 3	1301.60	± 14.53
Mode 5	3565.28	± 50.06
Mode 8	7050.83	± 85.19

3.2 FEA for defect build

The experimental testing was verified through FEA on one bar from each defect group. The details on each of the groups were provided after the experimental testing results were shown to the project sponsor. The defect size in each group was provided as follows: Group 1 has nominal parts (0 intentional defect) with each subsequent group increasing by a 50 μm defect until Group 9 which has a 400 μm defect. From the experimental testing, the first four bending x-

axis modes were found to correspond with modes in the FEA results (Table 2 not all modes are shown). This indicates that the experimental testing was valid as there was at most a 1.1% error between the results.

The ninth mode was found to have the greatest difference between the nominal group and the 50 and 400 μm defects. This indicates that the first axial mode should be excited in order to differentiate the groups.

Mode No.	Frequency (Hz)						
	Exp. Testing Avg. All Groups	Group 1: Nominal	Group 2: 50 μm defect	Group 3: 400 μm defect	Difference in Group 1 & 2	Difference in Group 1 & 9	Mode shape
1st mode	205	203.22	202.72	202.43	0.5	0.79	Cantilever x-axis
3rd mode	1302	1291.5	1289.7	1290.2	1.8	1.3	2nd order bending x-axis
5th mode	3565	3530	3521.5	3520.3	8.5	9.7	3rd order bending x-axis
8th mode	7050	6972	6969.1	6966.8	2.9	5.2	4th order bending x-axis
9th mode		9754.8	9594.5	9538.4	160.3	216.4	1st axial

3.3 Nominal Bar Build

After the layer defect build evaluation, a nominal build plate was sent to MTU to evaluate the variation across the build plate and compare to the defect build. This plate was tested using the same procedure as the layer defect build. The nominal bar build had more variation in natural frequency in comparison to the defect build (Table 3). The range and variance increased as the frequency increased for both builds indicating similar phenomenon in both plates. This indicates there is too much variation in the build process to determine the layer defect using the current testing method, since all the nominal bars should have the same natural frequency.

Table 2: Range and variance for Group 1: Nominal bars compared to the same bars on the nominal build.

	Range (Hz)		Variance (Hz^2)	
	Nominal build	Group 1: Nominal	Nominal Build	Group 1: Nominal
Mode 1	2.78	0.67	0.9	0.05
Mode 3	17.87	4.84	34.98	2.96
Mode 5	41.02	16.69	187.08	34.87
Mode 8	89.94	28.4	883.68	103.66

3.4 FEA for Topology Optimized Brackets

The FEA for the topology optimized brackets was provided to MTU before the brackets were received. The FEA was performed out to the 8^{th} mode shape (Fig. 6). The largest motion for each of the modes appear to be in the ears of each of the brackets. This indicated that experimental testing should be performed on the ears. Another observation from the FEA results is that Bracket 1 and Bracket 3 appear to be similar as at least two of the mode shapes excite both

of these brackets. This indicates that Bracket 1 and Bracket 3 will have some of the same natural frequencies in the FRFs.

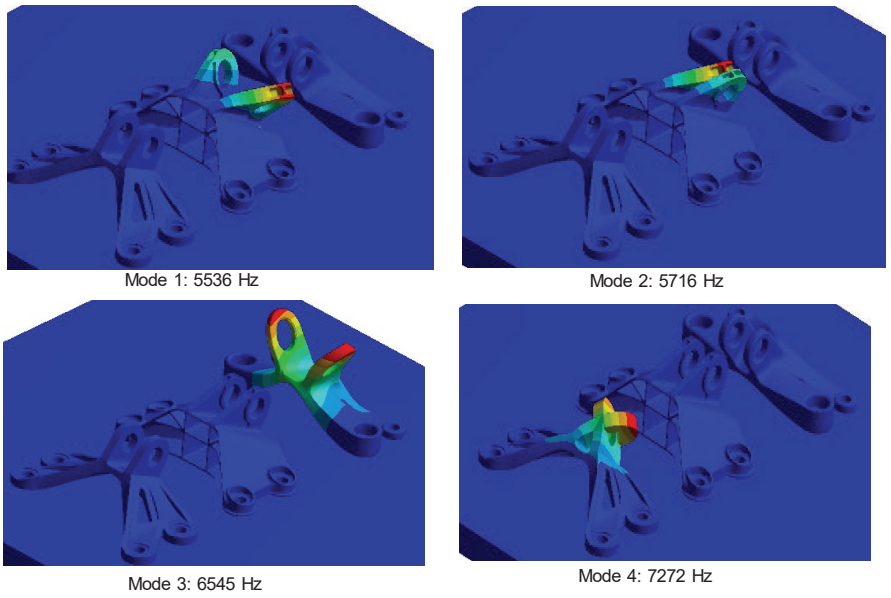

(6a)

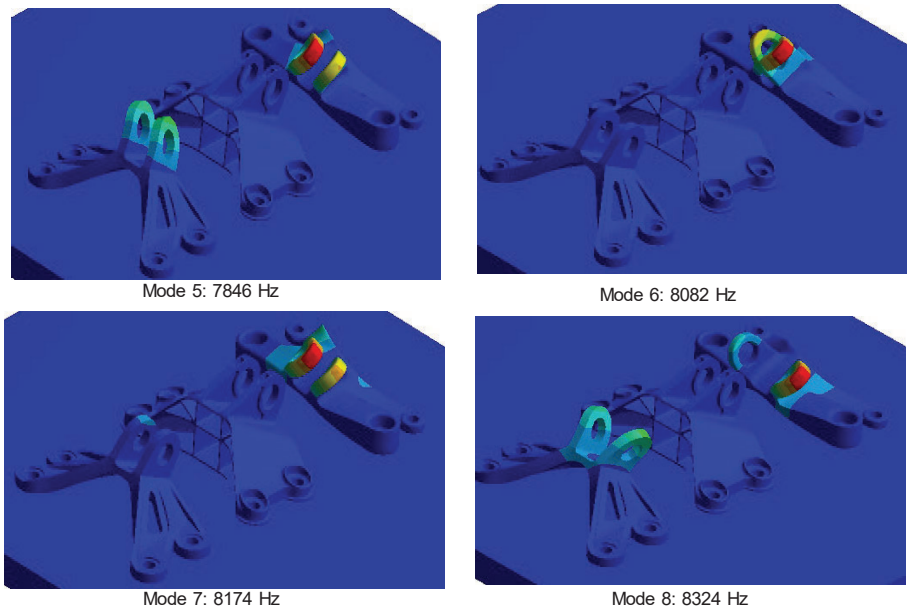

(6b)

Figure 6: First 4 mode shapes (6a) and last 4 mode shapes (6b) for topology optimized brackets from FEA provided by MS&T

3.5 Experimental Testing for Topology Optimized Brackets

The topology optimized brackets were tested in the same way as the nominal bar build to determine the natural frequencies of these parts and compare them to the FEA results. Only

results from Bracket 1 are shown as the other two brackets were unable to be tested, as there was not enough excitation for the SLDV to be able to detect the response. Also, the small impact hammer was switched for the large impact hammer, as the small hammer did not provide enough excitation. Analyzing the FRF, there are no distinct peaks in the band of interest (5500-8500 Hz) for these brackets as there is noise introduced above 4500 Hz (Fig. 7). Also, the coherence becomes noisy and starts to trend downward around ~4500 Hz indicating that the energy inputted into the structure is not being measured in the response. These two observations indicate that the impact hammer did not provide enough excitation to the structure to determine the natural frequencies. Therefore, there will be no comparison to the FEA from this testing.

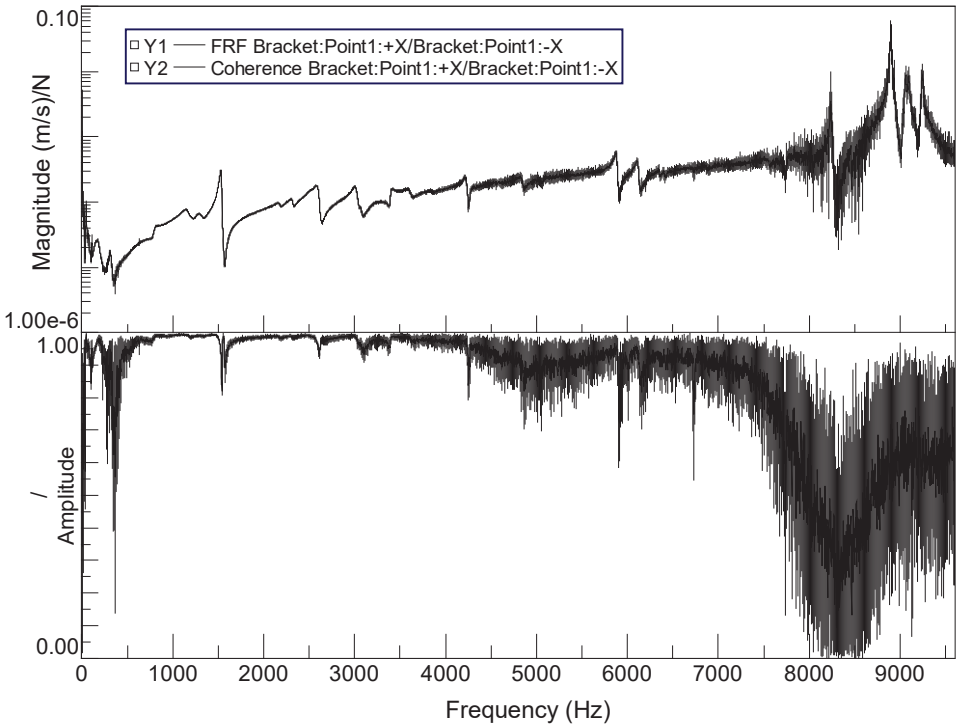

Figure 7: FRF and Coherence of Bracket 1

4. Discussion and Future Work

4.1 Discussion of Results

This paper presented investigations into determining if defect groups in AM parts could be determined from resonant frequency testing. From both the experimental testing and the FEA results of the forest bar builds the defect groups were not able to be distinguished from each other. Additionally, the topology optimized brackets were incomparable to the FEA since the resonant frequency test did not supply enough energy to the structure. A surprising finding was that the nominal build had more variation than the build with defects. In comparison to the study done by Johnson et al. the results in this study do not agree.

The nominal build having more variation than the defect build was surprising. One hypothesis on why this occurred is that unintentional defects were introduced in the printing

process. A second hypothesis is that the bars had more coupling and interference with the surrounding bars when being tested than originally expected since, even with the weights, there was a high level of variation in the parts.

The results from this study do not agree with the results from the chimney builds tested by Johnson et al., where they were able to determine which chimney had defects from a blind test. The difference in results between these two studies could be due to Johnson et al. investigating parts with much lower natural frequencies (less than 4000 Hz) with the parts being less complex and fewer in number per build in comparison to this study. The results in this paper suggest that impact hammer excitation may be suitable for lower frequencies, but may not be suitable for parts with higher natural frequencies or increased complexity.

4.2 Future Work

Future testing for these parts will be aimed at providing more energy to both the forest plate builds and the topology optimized brackets. A testing technique that may be suitable on the forest plate builds is acoustic excitation in the axial direction, as this is the mode that will be most likely to distinguish the defects from one another. Additionally, ultrasonic testing may be suitable for testing these builds, but tends to be more costly and time consuming. The topology optimized brackets future testing will be focused on firing a high velocity projectile via a BB - gun at the ears in order to provide energy over 5500 Hz to the structure.

5. Conclusion

In summary, the results from the investigations in this study were not able to determine the defect groups in the forest bar builds nor provide enough excitation to the topology optimized brackets to be able to compare to the FEA results. These findings suggest that resonant frequency inspection may not be suitable for testing parts with high natural frequencies. Therefore, other excitation techniques need to be investigated in future testing. Future testing may involve acoustic excitation, ultrasonic excitation, or high velocity projectile testing.

6. Acknowledgements

This work was funded by Honeywell Federal Manufacturing & Technologies under Contract No. DE-NA0002839 with the U.S. Department of Energy. The United States Government retains and the publisher, by accepting the article for publication, acknowledges that the United States Government retains a nonexclusive, paid up, irrevocable, world-wide license to publish or reproduce the published form of this manuscript, or allow others to do so, for the United States Government purposes.

References

[1] A. Karme, A. Kallonen, V.-P. Matilainen, H. Piili, and A. Salminen, "Possibilities of CT Scanning as Analysis Method in Laser Additive Manufacturing," *Physics Procedia*, vol. 78, pp. 347–356, 2015.

[2] NIST, "Measurement Science Roadmap for Metal-based Additive Manufacturing," *Energetics,* 2013, https://www.nist.gov/sites/default/files/documents/el/isd/NISTAdd_Mfg_Report_FINAL-2.pdf

[3] K. Johnson, J. Blough, and A. Barnard, "Frequency Response Identification of Additively Manufactured Parts for Defect Identification," in *Annual International Solid Freeform Fabrication Symposium*, August 2018, Austin, TX [Online]. Available: http://sffsymposium.engr.utexas.edu/archive. [Accessed: 07 Mar. 2019]

[4] B. J. Schwarz, "Experimental Modal Analysis," CSI Reliability Week, *Vibrant Technology, Inc.* Oct. 1999.